CHAPTER 201

WAVE OVERTOPPING RATE AND REFLECTION COEFFICIENT FOR OBLIQUELY INCIDENT WAVES

Yoichi MORIYA[1] and Masaru MIZUGUCHI[2]

Abstract

Recently, wave overtopping over a vertical wall for normal incidence were treated analytically on the basis of the wave energy flux concept (Mizuguchi, 1993). In this study, the Mizuguchi's model for normal incidence is extended to oblique incidence. Incident wave angle effect on the wave overtopping rate is investigated. Validity of the extended model is checked experimentally. Satisfactory agreement between the extended model and the experimental results was found for the wave overtopping rate.

1. Introduction

Wave overtopping for oblique incidence has been studied experimentally in several papers. The influence of the incident wave angle on wave overtopping tests over a vertical wall was studied by using regular waves by Inoue and Tuchiya (1971) or using irregular waves by Takayama et al. (1984). Recently, several model tests have been performed, for example, de Waal and van der Meer (1992) ; Juhl and Sloth (1994), and so on. However, the quantitative estimation of wave overtopping rate does not agree among the previous studies. The disagreement partly comes from the varying wave height in front of the wall.

Recently, for normal incidence, a set of simple equation to estimate the wave overtopping rate over a vertical wall and the reflection coefficient were derived

[1]Research Engineer; Penta-Ocean Construction Co., Ltd., Institute of Technology, Yonkucyo 1534-1, Nishinasuno-machi, Nasugun, Tochigi-Prefe., 329-27, JAPAN
[2]Professor; Dept. Civil Eng., Chuo Univ., Kasuga 1-13-27, Bunkyo-ku, Tokyo, 112, JAPAN

(Mizuguchi, 1993). The model, which does not include any experimental constants, is based on the energy flux concept with an assumption of partially standing waves. The validity of the model was confirmed by experiment (Yokoyama and Mizuguchi, 1993).

The purpose of this study is to investigate the influence of the incident wave angle on wave overtopping rate and reflection coefficient, by extending the model for normal incidence to oblique incidence. Validity of the extended model is checked experimentally.

2. Theoretical Approach

Wave field in front of vertical wall for oblique incidence

Figure 1 shows the coordinate system. When oblique waves incident a vertical wall, wave field in front of the vertical wall fully apart from the wall end is free from scattering waves forms bi-directional wave field. We supposed that wave field is uniform along the wall.

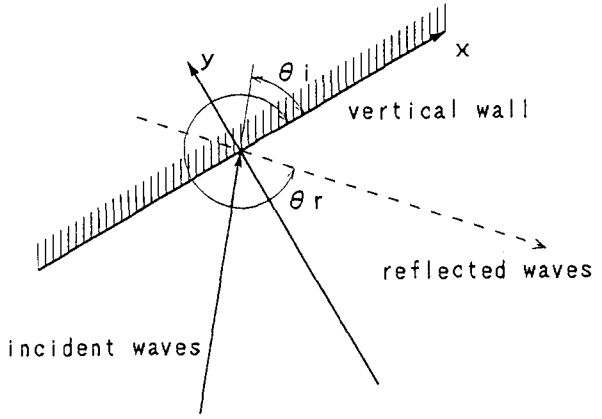

Figure 1 Coordinate system.

A finite amplitude wave theory is needed in evaluating the overtopping rate for waves with large height, especially in estimating the threshold wave height for overtopping. Since coastal structure are normally built in shallow water areas, the wave theory to be employed is the linear superposition of the first order cnoidal waves. The interaction between the incident waves and the reflected waves may be negligible as the interaction time is short. Surface elevation η in front of the vertical wall may be given by following formula:

$$\eta = \eta_i + \eta_r \tag{1}$$

$$= \frac{H_i}{2}\left[cn^2(\varphi_i;\kappa) - \overline{cn}\right] + \frac{H_r}{2}\left[cn^2(\varphi_r;\kappa) - \overline{cn}\right] \tag{2}$$

in which φ is the phase:

$$\varphi_j = \frac{K(\kappa)}{\pi}\left\{kx\cos\theta_j + ky\sin\theta_j - \sigma t\right\} \qquad j=i,r \tag{3}$$

where, H is the wave height, k is the wave number, σ is the angular frequency, θ is the wave angle, K(κ) is the complete elliptic integral of the first kind of modulus κ . The symbols cn denotes Jacobian elliptic function with modulus κ , and an overbar represents the average value over one period. The subscript i and r denote the quantity of the incident waves and the reflected waves, respectively.

Horizontal velocities of x and y direction, u and v, in front of the wall may be given by following formula:

$$u = \sqrt{\frac{g}{h}}\left(\eta_i\cos\theta_i + \eta_r\cos\theta_r\right) \tag{4}$$

$$v = \sqrt{\frac{g}{h}}\left(\eta_i\sin\theta_i + \eta_r\sin\theta_r\right) \tag{5}$$

where, g is the gravitational acceleration and h is the water depth.

Wave overtopping

Figure 2 shows schematic illustration of the wave overtopping over a vertical wall. For normal incidence, wave overtopping discharge is evaluated using an ideal fluid flow model over a sharp-edge weir by Kikkawa et al. (1967). When oblique waves are incident on a vertical wall, surface rise of the wave crest progresses along the wall. Wave overtopping for oblique incidence is supposed to be a kind of overflow of the surface rises over the wall. Then wave overtopping discharge, q_e, for oblique incidence averaged over one wave period may be given by following formula:

$$q_e = \frac{2\sqrt{2g}}{3T}\int_{\eta_e > H_c}\left\{\left(\frac{v_w^{\,2}}{2g} + \eta_e - H_c\right)^{\frac{3}{2}} - \left(\frac{v_w^{\,2}}{2g}\right)^{\frac{3}{2}}\right\}dt \tag{6}$$

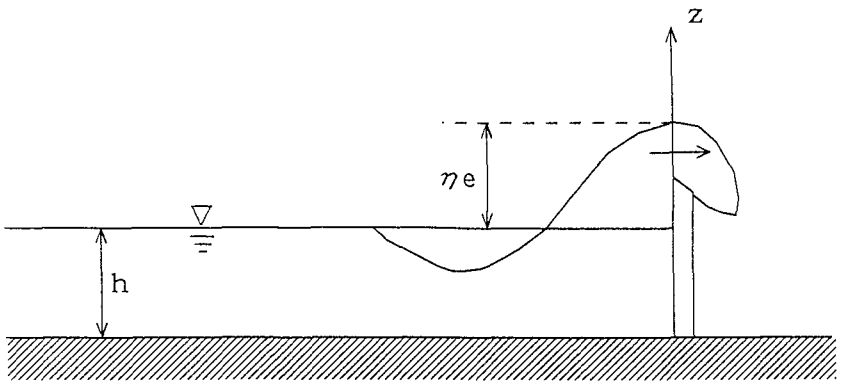

Figure 2 Schematic illustration of wave overtopping over a vertical wall.

where, T is the wave period, H_c is the crown height of the vertical wall above the still water level, η_e is the overtopping waves at the wall (η at y = 0) and v_w is the approaching velocity perpendicular to the wall.

Energy flux conservation

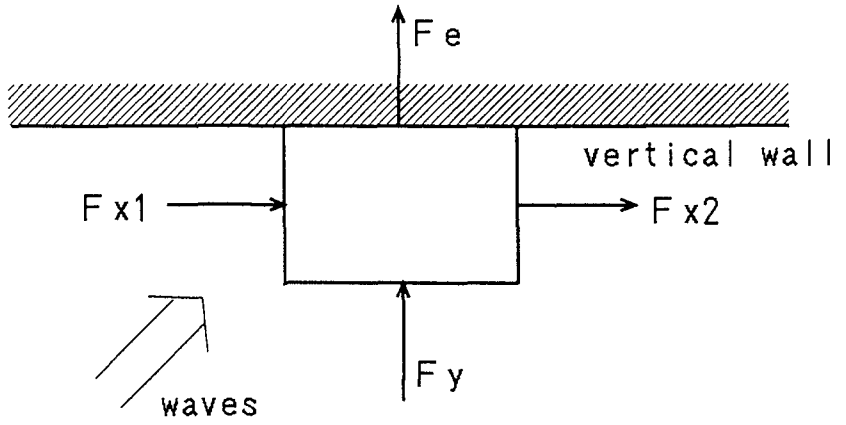

Figure 3 Schematic illustration of the energy flux conservation.

We consider the balance of the energy flux among the incident waves, the reflected waves and the wave overtopping flow. Figure 3 shows schematic illustration of wave energy

flux conservation. Here, F_x and F_y are the energy flux of x and y direction and F_e is the energy loss due to overtopping. We assume that the phenomenon of x direction (along the wall) is uniform, so the balance of energy flux yields following formula:

$$E_i c_g \sin\theta_i + E_r c_g \sin\theta_r = F_e \tag{7}$$

or

$$f_{2i} H_i^{\,2} \sin\theta_i - f_{2r} H_i^{\,2} K_r^{\,2} \sin\theta_i = \frac{2\sqrt{2g}}{3T\sqrt{h}} \int_{\eta_e > H_c} \left\{ \left(\frac{v_w^{\,2}}{2g} + \eta_e - H_c \right)^{\frac{3}{2}} - \left(\frac{v_w^{\,2}}{2g} \right)^{\frac{3}{2}} \right\} \left(\eta_e + \frac{1}{2g} \left| u_w^{\,2} + w_w^{\,2} \right|_{z=0} \right) dt \tag{8}$$

where, K_r is the reflection coefficient defined as the wave height ratio and u_w is the velocity along the wall. f_2 is the ratio between the energy and the wave height square on the first order cnoidal wave theory (Isobe, 1985), and is 1/8 for the small amplitude wave theory.

Equation (8) gives the reflection coefficient, when incident wave height, period and angle are prescribed together with geometry or the freeboard of the vertical wall. The wave overtopping discharge can be estimated from eq. (6) by using the reflection coefficient.

Numerical calculation

We performed numerical calculation of this model. We examine the influence of the incident wave angle and the incident wave height while water depth 20.0 cm and wave period 1.2 s are kept constant.

Figure 4 shows examples of the calculated non-dimensional overtopping rate q_e/q_0 and reflection coefficient K_r with respect to incident wave angle. Wave overtopping discharge, q_e, is non-dimensionalized with q_0 defined as

$$q_0 = \frac{H_i \sqrt{gh}}{2}. \tag{9}$$

We performed the calculation using not only the first order cnoidal wave theory but also the small amplitude wave theory. It is clear that the wave overtopping rate and the reflection coefficient slightly decrease with the decrease of the incident wave angle. Significant decreases of more than 10%

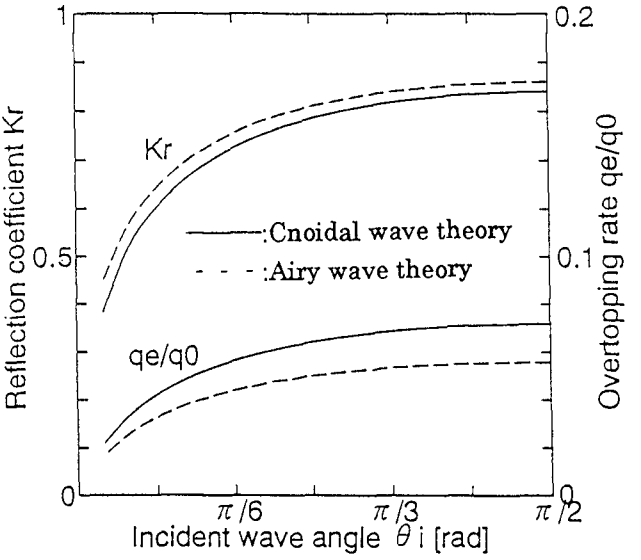

Figure 4 Examples of the calculated non-dimensional overtopping rate q_e/q_0 and reflection coefficient K_r with respect to incident wave angle.(calculation condition h=20cm,T=1.2s,H_i=6cm,H_c=3cm)

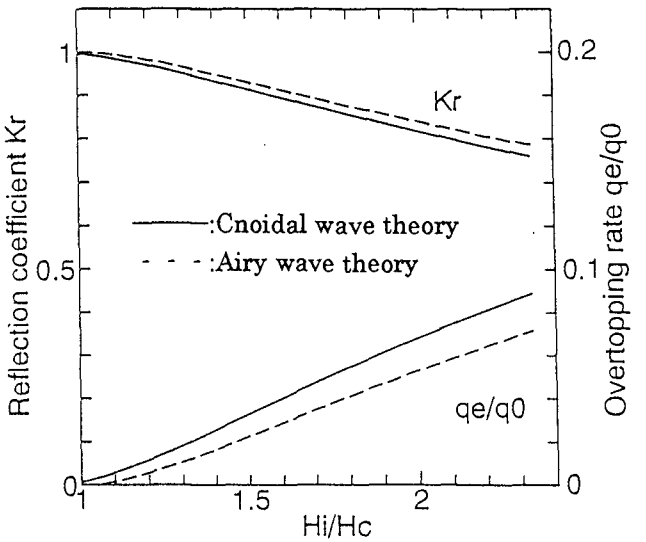

Figure 5 Examples of the calculated non-dimensional overtopping rate q_e/q_0 and reflection coefficient K_r with respect to incident wave height.(calculation condition h=20cm,T=1.2s,$\theta_i=\pi/3$,H_c=3cm)

are expected only for the incident wave angle less than π /4. Nonlinear effect yields the increase of the overtopping rate and the decrease of the reflection coefficient.

Figure 5 shows examples of the calculated non-dimensional overtopping rate q_e/q_0 and reflection coefficient K_r with respect to incident wave height. The difference between for the small amplitude waves and for the cnoidal waves in the overtopping rate and the reflection coefficient becomes larger as the incident wave height gets larger.

3. Experimental Confirmation

Experimental facilities

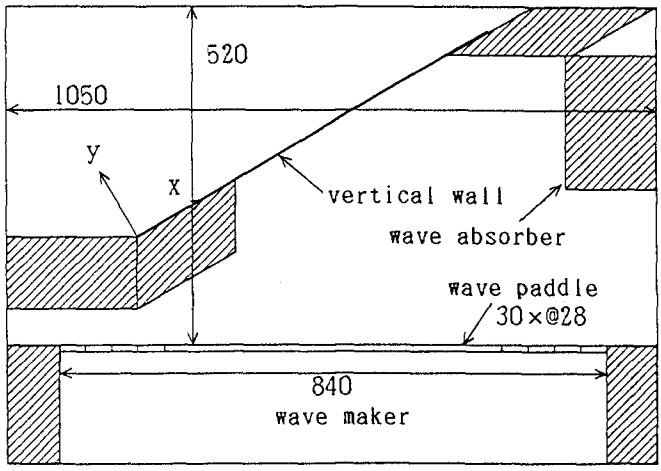

unit:cm

Figure 6 Experimental facilities and the coordinate system.

Experimental confirmation of this model is undertaken by using a multi-directional wave basin. Figure 6 shows the experimental facilities and the coordinate system. The basin is 10.5 m wide, 6.8 m long and 0.6 m depth. The distance from wave paddles to opposite end-wall is 5.2 m. The concrete floor of the basin is almost flat. The multi-directional wave maker consists of 28 piston-type wave paddles continuously linked or 29 sets of actuator rod. Each paddle is 30 cm wide and 50 cm high.

A vertical wall with 12.0 cm high and 540 cm long is installed in the basin. The influence of the scattering waves from the wall ends may be suppressed by placing wave absorbers around the wall ends.

In a multi-directional wave basin, generating a uniform wave field with the target value of wave height and angle is important. However, it is well known that both wave height and angle of generated regular waves show considerable spatial variation. The main cause is the finite length of the wave maker. The effect of the discontinuity at both ends of the wave maker may be suppressed by employing linear decrease of wave paddle amplitude (Mizuguchi, 1994). We applied this ends control method.

Water depth h = 10.0 cm, the crown height of the wall H_c = 2.0 cm, and a wave period of T = 1.0 s are kept constant. Incident wave height and incident wave angle are varied.

Wave field in front of the wall

Non-overtopping experiments (incident wave height H_i =1.0 cm) were carried out in order to check the uniformity of the wave field in front of the vertical wall. Wave gauges are installed 1.0 cm distant perpendicularly to the wall. An array of wave gauge and electro-magnetic current meter measures the surface elevation and the horizontal velocity at the same point 1/12 of wave length perpendicularly apart from the wall.

Figure 7 shows the wave height and the total amplitude of the horizontal velocity distribution in front of the vertical wall for non-overtopping cases. Wave field in front of the wall can be assumed to be uniform at the center of the wall. Where we measure wave overtopping discharge for all the cases.

Separation method between incident and reflected waves

A separation method is developed to evaluate the reflection coefficient and the reflected wave angle from the measured data. The method assumes the linear superposition of the incident waves and the reflected waves, both of them being long waves.

Mathematically, we have eq. (10), eliminating η_i and η_r from eqs. (1), (4) and (5),

$$\frac{\sqrt{h/g}u-\eta\cos\theta_i}{\sqrt{h/g}v-\eta\sin\theta_i}=\frac{\cos\theta_r-\cos\theta_i}{\sin\theta_r-\sin\theta_i}=\alpha \qquad (10)$$

where, α is theoretically a constant, although α vary for a measured data. Symmetrical reflection ($\theta_r = 2\pi - \theta_i$) gives $\alpha = 0$. Incident waves and reflected waves are calculated by following formula,

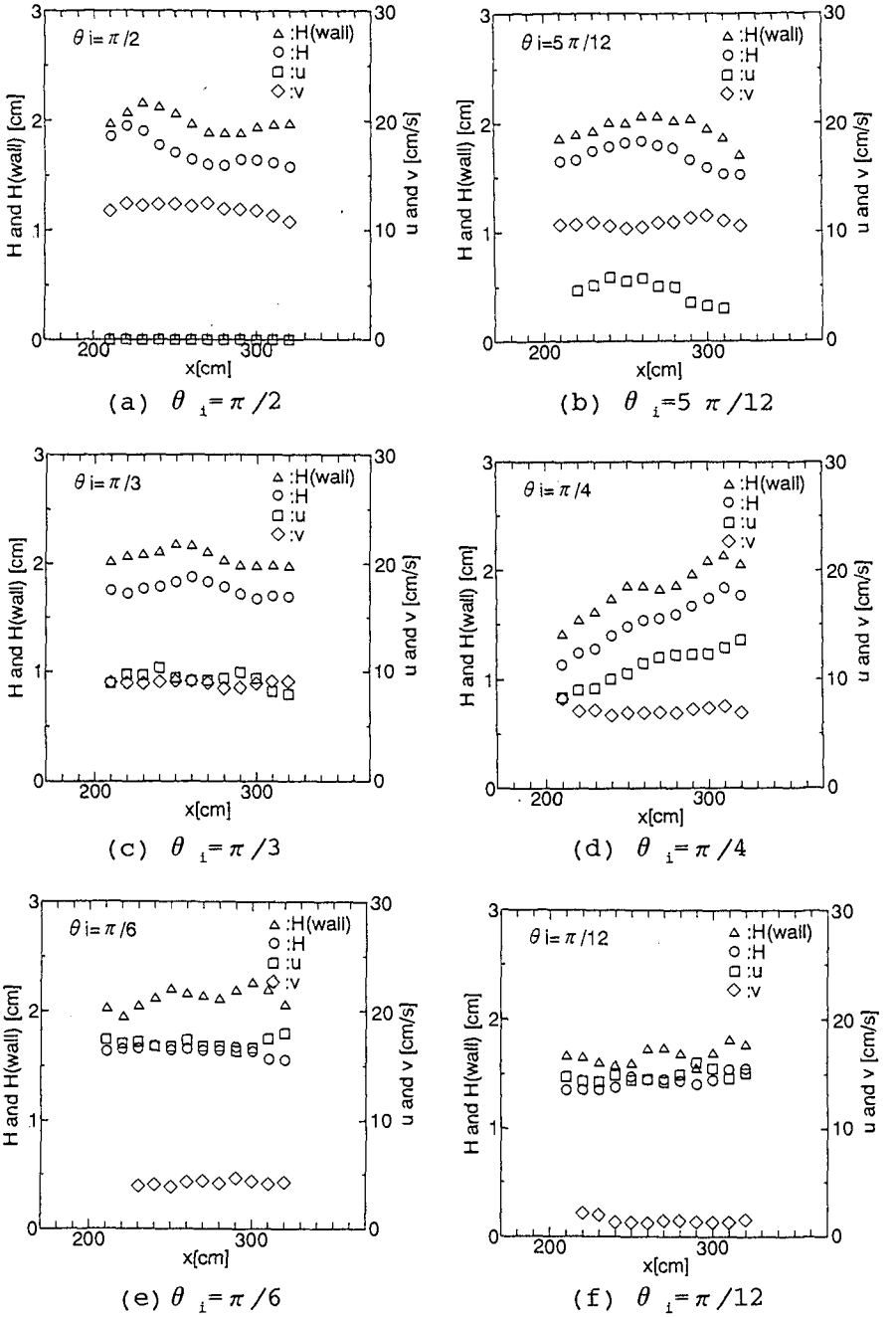

Figure 7 Wave height and total amplitude of horizontal velocity distribution in front of the wall.

$$\eta_i = \frac{\sqrt{h/g}v - \eta\sin\theta_r}{\sin\theta_i - \sin\theta_r}\left(= \frac{\sqrt{h/g}u - \eta\cos\theta_r}{\cos\theta_i - \cos\theta_r}\right) \tag{11}$$

and

$$\eta_r = \eta - \eta_i . \tag{12}$$

Reflection coefficient is the ratio between the incident wave height and the reflected wave height.

Wave overtopping rate and reflection coefficient

Incident wave heights are H_i = 2.0, 2.5, 3.0 and 3.5 cm in wave overtopping experiments. The wave overtopping discharge are measured by using a wave gauge in the box installed just behind the wall.

Figure 8 shows examples of measured data of surface elevation η and horizontal velocities u and v. Figure 9 shows separated incident waves and reflected waves calculated from equation (10) and (11) together with the time series of α, as using data shown in Fig. 8. Reflected wave angle is calculated by using mean value of α passed from -1 to 1.

Figure 10 shows reflected wave angle obtained from experimental data. When incident wave angle is large, the reflected wave angle shows almost symmetry. However, when incident wave angle is small, the reflected wave angle shows large discrepancy from symmetrical reflected angle. We may consider the reason why the separation method for incident and reflected waves suffers strongly influence from experimental noise. Figure 11 shows incident wave height obtained from experimental data. Incident wave height is almost the same as the target value. When incident wave angle is large, the validity of the separation method was confirmed.

Figure 12 shows measured and calculated wave overtopping rates and reflection coefficients with respect to the incident wave angle. Wave overtopping was not observed, for incident wave height H_i = 2 cm of all incident wave angles and H_i = 2.5 cm of incident wave angle $\theta_i = \pi/4$, $\pi/6$ and $\pi/12$. When wave overtopping occurs, good agreement between the model and the experiment results is found for the wave overtopping rate. The reflection coefficients for large incidence ($\theta_i = \pi/2$, $5\pi/12$ and $\pi/3$) show reasonable values. For small incident wave angle, the reflection coefficient obtained from experimental data did not plot.

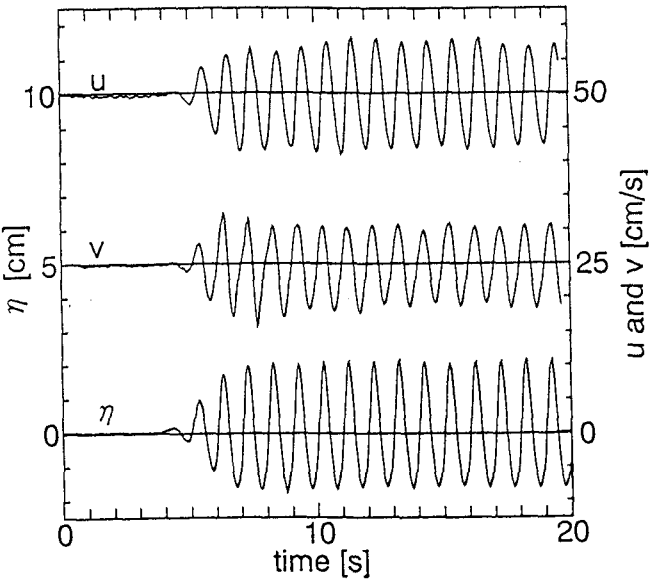

Figure 8 Examples of measured data of surface elevation η and horizontal velocities u and v.(h=10cm,T=1.0s,H_i=3.0cm, $\theta_i = \pi/3$)

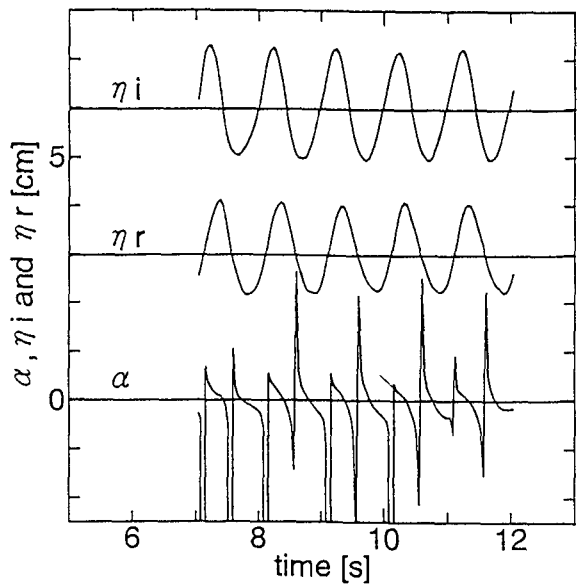

Figure 9 Time series of α, separated incident waves and reflected waves calculated as using data shown in Fig. 6.

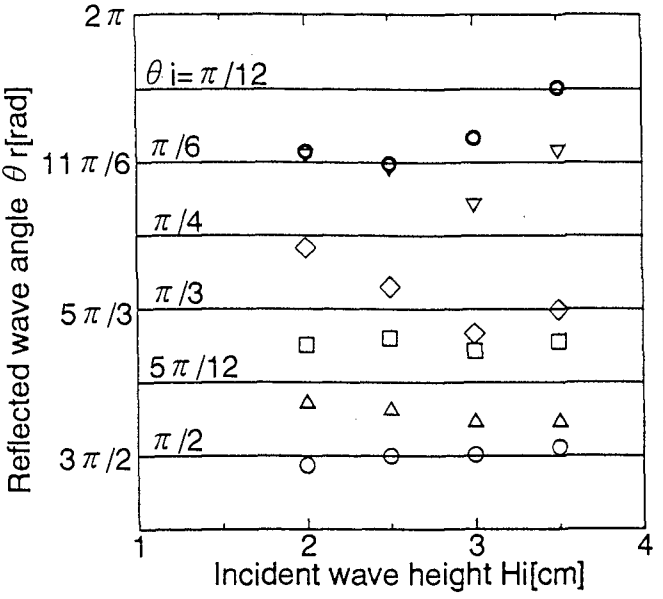

Figure 10 Reflected wave angle obtained from experimental data.(○: $\theta_i=\pi/2$, △:5 $\pi/12$, □: $\pi/3$, ◇: $\pi/4$, ▽: $\pi/6$, ◎: $\pi/12$)

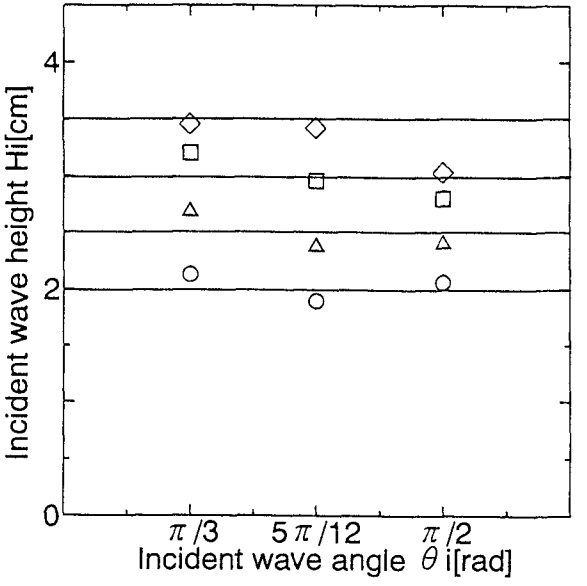

Figure 11 Incident wave height obtained from experimental data.(○:H_i=2.0cm, △:2.5cm, □:3.0cm, ◇:3.5cm)

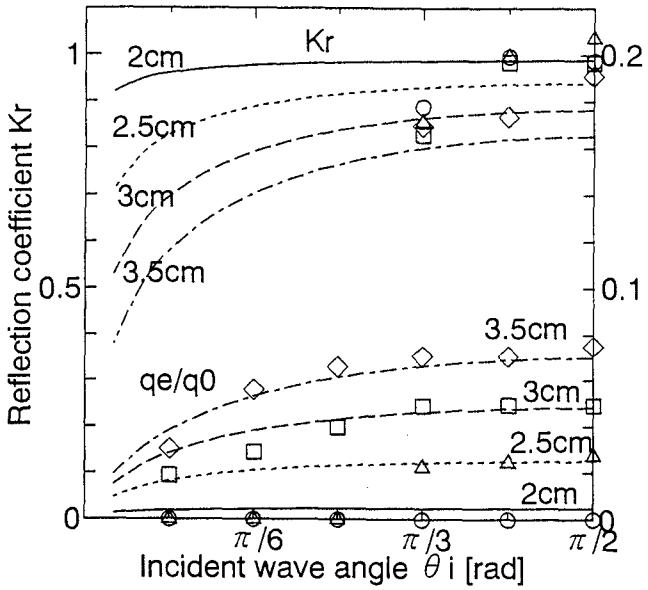

Figure 12 Measured and calculated wave overtopping rates and reflection coefficients with respect to the incident wave angle. (○:H_i=2.0cm,△:2.5cm,□:3.0cm,◇:3.5cm)

4. Conclusion

Wave overtopping over a vertical wall for the oblique incidence were treated analytically by extending normal incidence (Mizuguchi's) model. Wave overtopping rate and reflection coefficient can be estimated from the extended model which does not include any experimental constants. The results of numerical calculation show the slightly decrease of the wave overtopping rate with the decrease of the incident wave angle.

Experimental confirmation of this model was undertaken by using a multi-directional wave basin. Satisfactory agreement between the model and the experimental results is found for the wave overtopping rate. The reflection coefficient for large incidence ($\theta_i = \pi/2, 5\pi/12$ and $\pi/3$) shows reasonable agreements. The validity of the model was confirmed at least for large incident wave angle.

Reference

de Waal, J. P. and J. W. van der Meer(1992):Wave runup and overtopping on coastal structures, Proc. 23rd, Conf.

Coastal Eng., ASCE, pp.1758-1771.
Inoue, M. and Y. Tuchiya(1971): Experimental study on wave overtopping over a vertical wall for oblique incidence, Proc, 18th, Japanese Conf. on Coastal Eng., JSCE, pp.259-264. (in Japanese)
Isobe, M.(1985): Calculation and application of first order cnoidal wave theory, Coastal Eng., Elsevier, Vol.9, pp.309-325.
Juhl, J. and P. Sloth(1994): Wave overtopping of breakwaters under oblique waves, Proc. 24th, Conf. Coastal Eng., ASCE, pp.1182-1196.
Kikkawa, H., H. Shiigai and T. Kohno(1967): Basic study on wave overtopping for coastal embankment (1), Proc. 14th, Japanese Conf. on Coastal Eng., JSCE, pp.335-338. (in Japanese)
Mizuguchi, M.(1993): Wave overtopping rate over a vertical wall and reflection coefficient, Coastal Eng. in Japan, Vol.36, No.1, pp.37-47.
Mizuguchi, M.(1994): Uniformity of wave field produced by multi-directional wave maker, Abst. 24th, Conf. Coastal Eng., ASCE.
Takayama, T., T. Nagai, K. Nishida and T. Sekiguchi(1984): Experiments on oblique random wave overtopping rates over seawalls, Proc. 31st, Japanese Conf. on Coastal Eng., JSCE, pp.542-546. (in Japanese)
Yokoyama, K. and M. Mizuguchi(1993): Experimental study on wave overtopping over a vertical wall and reflection coefficient, Proc. Coastal Eng., JSCE, Vol.40, pp.676-680. (in Japanese)